

# <sup>13</sup>C flux analysis of cyanobacterial metabolism

Adeola O. Adebisi · Lara J. Jazmin ·  
Jamey D. Young

Received: 14 April 2014 / Accepted: 22 September 2014 / Published online: 4 October 2014  
© Springer Science+Business Media Dordrecht 2014

**Abstract** <sup>13</sup>C metabolic flux analysis (MFA) has made important contributions to our understanding of the physiology of model strains of *E. coli* and yeast, and it has been widely used to guide metabolic engineering efforts in these microorganisms. Recent advancements in <sup>13</sup>C MFA methodology combined with publicly available software tools are creating new opportunities to extend this approach to examine less characterized microbes. In particular, growing interest in the use of cyanobacteria as industrial hosts for photosynthetic production of biofuels and biochemicals has led to a critical need to better understand how cyanobacterial metabolic fluxes are regulated in response to changes in growth conditions or introduction of heterologous pathways. In this contribution, we review several prior studies that have applied isotopic steady-state <sup>13</sup>C MFA to examine heterotrophic or mixotrophic growth of cyanobacteria, as well as recent studies that have pioneered the use of isotopically nonstationary MFA (INST-MFA) to study autotrophic cultures. We also provide recommendations for the design and analysis of INST-MFA experiments in cyanobacteria, based on our previous experience and a series of simulation studies used to assess the selection of measurements and sample time points. We anticipate that this emerging knowledgebase of prior <sup>13</sup>C MFA studies, optimized experimental protocols, and public

software tools will catalyze increasing use of <sup>13</sup>C MFA techniques by the cyanobacteria research community.

**Keywords** Metabolic flux analysis · Cyanobacteria · Isotope labeling experiment · Optimal experiment design · Isotopically nonstationary MFA

## Abbreviations

2PG	2-Phosphoglycolate
3PGA	3-Phosphoglycerate
ACA	Acetyl CoA
AKG	α-Ketoglutarate
ALA	Alanine
ARG	Arginine
ASN	Asparagine
ASP	Aspartate
CIT	Citrate
CO <sub>2</sub>	Carbon dioxide
CYS	Cysteine
E4P	Erythrose-4-phosphate
F6P	Fructose-6-phosphate
FBP	Fructose-1,6-bisphosphate
FUM	Fumarate
G1P	Glucose-1-phosphate
G6P	Glucose-6-phosphate
GA	Glycerate
GLC	Glycolate
GLN	Glutamine
GLU	Glutamate
GLY	Glycine
GLYC	Glycogen
GOX	Glyoxylate
HIS	Histidine
ICI	Isocitrate
ILE	Isoleucine

---

Guest Editor: Peter Lindblad.

---

A. O. Adebisi · L. J. Jazmin · J. D. Young  
Department of Chemical and Biomolecular Engineering,  
Vanderbilt University, Nashville, TN 37235, USA

J. D. Young (✉)  
Department of Molecular Physiology and Biophysics, Vanderbilt  
University, Nashville, TN 37235, USA  
e-mail: j.d.young@vanderbilt.edu

LEU	Leucine
LYS	Lysine
MAL	Malate
MET	Methionine
OAA	Oxaloacetate
PEP	Phosphoenolpyruvate
PHE	Phenylalanine
PRO	Proline
PYR	Pyruvate
R5P	Ribose-5-phosphate
RU5P	Ribulose-5-phosphate
RUBP	Ribulose-1,5-bisphosphate
S7P	Sedoheptulose-5-phosphate
SBP	Sedoheptulose-1,7-bisphosphate
SER	Serine
SUC	Succinate
THR	Threonine
TP	Triose phosphates, dihydroxyacetone phosphate and glyceraldehyde-3-phosphate
TRP	Tryptophan
TYR	Tyrosine
VAL	Valine
X5P	Xylulose-5-phosphate

## Introduction

Metabolic flux analysis (MFA) is a mathematical modeling approach that can be used to comprehensively determine the steady-state flow of material through intracellular biochemical pathways (Sauer 2006; Wiechert 2001; Stephanopoulos 1999; Nielsen 2003). The final outcome of MFA is a metabolic flux map, which is essentially a traffic diagram that depicts the *in vivo* activity of metabolic enzymes. This information can be used to identify major intracellular pathways and critical branch points in the metabolic network, to calculate rates of otherwise unmeasurable pathways, and to determine maximum theoretical yields for synthesis of products or biomass from complex, integrated biochemical pathways (Woolston et al. 2013). However, MFA is most useful when flux comparisons can be made between different strains or growth conditions and also when combined with other ‘-omics’ datasets. This enables researchers to understand flux control at metabolic branch points (Vallino and Stephanopoulos 1994), identify kinetic or regulatory bottlenecks in the metabolic network (Antoniewicz et al. 2007b), and identify targets for re-routing flux to desirable end products (or away from wasteful byproducts). One classic example that illustrates the application of MFA for selection of metabolic engineering targets is the overproduction of lysine in the soil

bacterium *Corynebacterium glutamicum*, which has been expertly summarized by Koffas and Stephanopoulos (2005).

MFA begins with the translation of available biochemical and genomic information into a set of mathematical equations representing metabolite mass balances, which can be augmented by various thermodynamic and/or regulatory constraints. Stoichiometric MFA approaches apply these balance equations to solve for intracellular fluxes based on measurements of extracellular substrate consumption or product formation rates. However, the system of mass balance equations is typically underdetermined for realistic metabolic networks, and therefore, it is not possible to solve for all intracellular fluxes without making additional ad hoc assumptions. In this case, optimization-based or constraint-based methods are often applied to explore the space of possible solutions, rather than attempting to identify a unique flux solution. Alternatively, additional measurements derived from isotope labeling experiments (ILEs) can be used to generate an overdetermined system of equations that can be solved using least-squares regression. This requires that the metabolic model is expanded to include isotopomer balances in addition to metabolite mass balances, which together provide the mathematical basis for  $^{13}\text{C}$  MFA calculations.

The elucidation of flux through reversible reaction steps, metabolic cycles, or parallel intracellular pathways cannot be accomplished using stoichiometric MFA unless these pathways are linked directly to measurable end products. This is an important consideration for the main pathways of interest in cyanobacteria: the Calvin–Benson–Bassham (CBB) cycle, the pentose phosphate pathway (PPP), the tricarboxylic acid (TCA) pathway and its associated anaplerotic pathways, and the glycolysis and gluconeogenesis pathways. These pathways serve to fix carbon dioxide into organic molecules and then redistribute that carbon to meet metabolic demands, but their flux is not directly coupled to the production of readily measurable sink compounds. However, since enzymes rearrange atoms in consistent and distinct patterns, feeding  $^{13}\text{C}$ -labeled substrates provides a way to distinguish flux contributions from different pathways based on the unique atomic rearrangements they produce. Metabolite labeling is measured using either nuclear magnetic resonance (NMR), which provides information on the position of labeled carbon atoms, or mass spectroscopy (MS), which offers greater sensitivity and throughput than NMR but less positional information. These isotope labeling data along with measured rates of substrate uptake and product formation provide experimental inputs that are used to regress the flux parameters defined in the  $^{13}\text{C}$  MFA model.

Two different  $^{13}\text{C}$  MFA approaches have been applied to cyanobacteria: steady-state MFA (SS-MFA) and

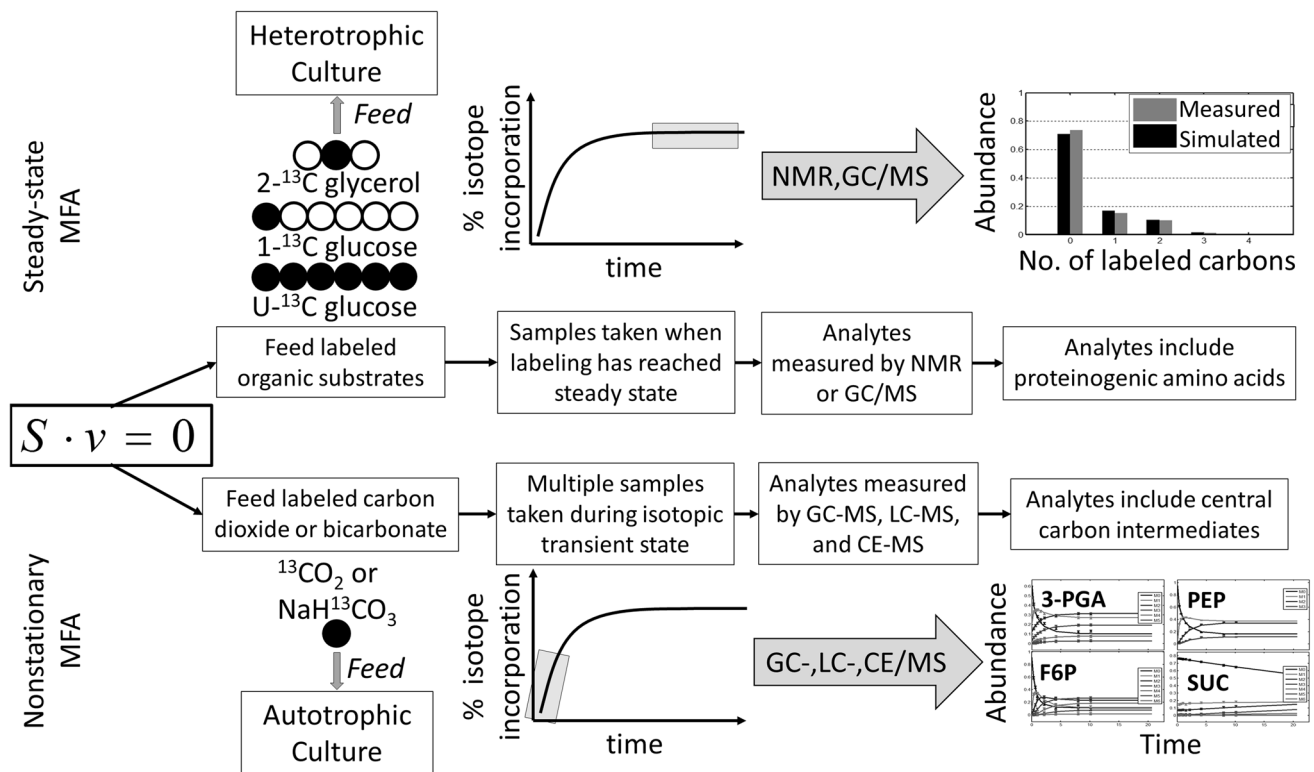


**Fig. 1** Two  $^{13}\text{C}$  MFA approaches applied to cyanobacteria. MFA begins with a set of mass balances describing a cell culture at metabolic steady state. Feeding a  $^{13}\text{C}$  tracer and measuring isotopomer abundances of intracellular metabolites can provide additional information to constrain the flux solution. This involves least-squares regression based on an expanded model that includes both mass and

isotopomer balances. Heterotrophic cultures can be analyzed by performing steady-state MFA with labeling measurements obtained from  $^{13}\text{C}$ -labeled glucose or glycerol tracers. Autotrophic cultures, on the other hand, require transient  $^{13}\text{C}$  labeling experiments followed by INST-MFA.  $S$  stoichiometric matrix,  $v$  flux vector

isotopically nonstationary MFA (INST-MFA) (Fig. 1). The term “steady state” refers to isotopic steady state, which implies that labeling measurements are obtained after  $^{13}\text{C}$  incorporation into intracellular metabolites has fully equilibrated. Ideally, the experiment is performed in continuous culture to maintain metabolic steady state throughout the ILE; alternatively, exponential-phase batch cultures have been used to approximate metabolic steady-state conditions. The isotope tracer is typically a mixture of  $^{13}\text{C}$  labeled glucose analogs, the composition of which should be selected to maximize flux precision within the pathways of interest (Antoniewicz 2013). Cell biomass samples are harvested and hydrolyzed to measure  $^{13}\text{C}$  labeling in proteinogenic amino acids, chosen for their high intracellular abundance compared to free intracellular metabolites and for the distinct metabolic pathways represented by their carbon precursors (Fig. 2). Based on the assumptions of metabolic and isotopic steady state, the isotopomer balances form a system of algebraic equations that can be solved to simulate how isotope labeling depends on the flux parameters in the  $^{13}\text{C}$  MFA model. Sophisticated computational algorithms such as the

cumomer method and elementary metabolite unit (EMU) method have been introduced to solve these equations efficiently, which facilitate rapid flux estimation and statistical analysis, even in large metabolic networks (Wiechert et al. 1999; Araúzo-Bravo and Shimizu 2003; Antoniewicz et al. 2007a).

INST-MFA becomes necessary when the assumption of isotopic steady state is no longer valid. It is especially useful for studies of autotrophic metabolism, since feeding  $^{13}\text{CO}_2$  will eventually produce a uniform  $^{13}\text{C}$ -labeling pattern in all downstream metabolites, and therefore, steady-state labeling measurements do not reflect carbon atom rearrangements within the network (Shastri and Morgan 2007). However, transient measurements of isotope incorporation following a feed switch from natural  $\text{CO}_2$  to  $^{13}\text{CO}_2$  can be used to estimate autotrophic fluxes by applying INST-MFA (Young et al. 2011). Our lab has recently developed a package of MATLAB routines called INCA that automates the computational workflow of INST-MFA (Young 2014). This involves solving a coupled system of ordinary differential equations that comprises the transient isotopomer balances. INCA relies on the EMU

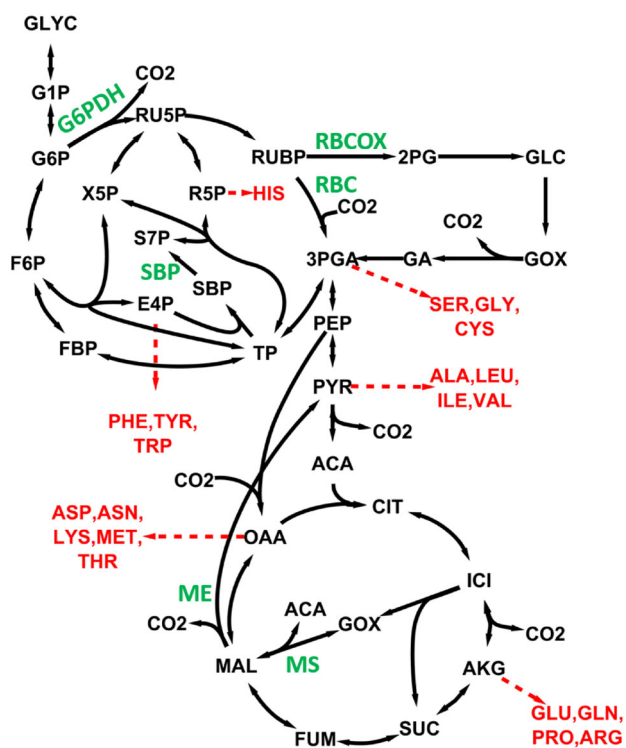


**Fig. 2** Proteinogenic amino acids used to inform SS-MFA calculations. These building blocks, highlighted in red, serve as proxies of central metabolic precursors. Their labeling patterns provide information about flux partitioning at several important metabolic branch points. Six independent net fluxes *G6PDH* glucose-6-phosphate dehydrogenase, *RBC* RuBisCO carboxylase, *RBCOX* RuBisCO oxygenase, *SBP* SBPase, *ME* malic enzyme, and *MS* malate synthase are shown for reference and highlighted in green

framework to efficiently simulate transient  $^{13}\text{C}$  labeling experiments (Young et al. 2008), making it the first publicly available software package that can apply INST-MFA to metabolic networks of arbitrary size and complexity. The experimental system must be maintained at metabolic steady state throughout the labeling time course, but the tracer experiments are performed on a time scale of minutes rather than hours in order to assess the dynamics of  $^{13}\text{C}$  incorporation. For this reason, isotopomer measurements obtained from proteinogenic amino acids are not useful for INST-MFA due to their slower rate of labeling. Instead, rapid sampling and cold-quenching of cells is required to fix the in vivo labeling state of central carbon metabolites, which can be measured in cell extract samples using a variety of mass spectrometry approaches (Jazmin and Young 2013; Jazmin et al. 2014).

Berla et al. (2013) have recently reviewed applications of stoichiometric MFA to cyanobacteria, and a number of other recent articles have reviewed applications of  $^{13}\text{C}$  MFA to examine general aspects of microbial metabolism (Matsuoka and Shimizu 2010; Tang et al. 2009). In this contribution, we first review prior applications of both SS-

MFA and INST-MFA to cyanobacteria as a way to highlight its utility for discovering novel metabolic functions in this important class of microbes. Then, we provide recommendations for design and analysis of INST-MFA studies of cyanobacteria, since this is an emerging area of research with few examples currently established in the literature. These recommendations are based on our prior experience with this technique as well as comprehensive in silico studies that have been performed to optimize the selection of measurements and sampling time points.

## Applications of $^{13}\text{C}$ MFA to cyanobacteria

### Steady-state $^{13}\text{C}$ MFA

Steady-state MFA was first applied to *Synechocystis* sp. PCC 6803 to investigate central carbon metabolism under mixotrophic and heterotrophic conditions (Yang et al. 2002a, b, c). The predominant mode of carbon utilization was determined by analyzing metabolites using a mixed feed of 90 % unlabeled glucose and 10 % fully labeled  $[\text{U-}^{13}\text{C}_6]$  glucose. Heterotrophic cells were found to utilize the oxidative PPP (oxPPP) almost exclusively for energy production, with more than 90 % of the incoming glucose metabolized by this pathway to produce NADPH for growth and respiration. The coupling of NADPH production to oxidative phosphorylation represents a unique respiratory pathway found in cyanobacteria and is believed to compensate for the lack of an intact cyanobacterial TCA cycle (Pelroy et al. 1972). Under mixotrophic conditions, Calvin cycle flux was approximately two-fold higher than glucose uptake, fueled by NADPH and ATP production from photosynthetic light reactions. However, flux through RuBisCO still only accounted for one-third of the total carbon uptake. The authors also noted a substantial cyclic flux through phosphoenolpyruvate carboxylase (PEPC) and malic enzyme (ME) under both heterotrophic and mixotrophic conditions, which is similar to the pathway of carbon assimilation found in C4 plants.

In addition to their  $^{13}\text{C}$  MFA studies, Yang et al. (2002a) compared mRNA transcript levels and protein expressions with pathway fluxes to decipher mechanisms of metabolic regulation. Consistent with their flux results, genes encoding phycobilisomes, RuBisCO, and the Calvin-cycle-associated *gap2* isoform of glyceraldehyde-3-phosphate dehydrogenase (GAPDH) were all transcriptionally repressed under heterotrophic conditions, while the oxPPP gene *gnd* was upregulated by about 60 %. Conversely, some expression levels did not appear to be in agreement with the flux results, indicating post-translational regulation by cellular redox or metabolite concentrations. For example, several genes encoding enzymes of central

carbon metabolism including *prk*, *zwf*, *gap1*, *fbp*, *pfkA*, *fbxA*, *fda*, *glk*, *cfxE*, *ppc*, *icd*, and *citH* were largely unaffected by light at the transcriptional level despite dramatic rerouting of flux through these pathways. This work highlights the utility of  $^{13}\text{C}$  MFA to uncover novel insights about regulatory mechanisms when combined with other ‘-omics’ platforms.

Nakajima et al. (2014) combined  $^{13}\text{C}$  MFA with metabolomics and transcriptomics analysis of *Synechocystis* to compare cells grown under mixotrophic conditions and photoheterotrophic conditions. Labeling was achieved by an optimized 0.7:0.3 mix of  $[1-^{13}\text{C}]$  glucose and  $[\text{U}-^{13}\text{C}_6]$  glucose while atrazine was added to the photoheterotrophic cultures to inhibit photosynthesis. Samples were taken during the exponential growth phase, and nine proteinogenic amino acids were selected for analysis: alanine, aspartate, glutamate, phenylalanine, glycine, isoleucine, leucine, serine, and valine. A comparison of the fluxes and their 95 % confidence intervals showed that over half of the fluxes differed significantly between the two culture conditions. Changes in enzyme expression within these pathways were less dramatic, with most genes differing by less than two-fold between mixotrophic and photoheterotrophic conditions. A six-fold increase in RuBisCo flux was observed under mixotrophic conditions when compared to photoheterotrophic conditions. However, there was no significant change in the levels of RU5P or ribulose-1,5-bisphosphate (RUBP) or expression of *prk*, *rbcL*, or *rbcS*. OxPPP flux was elevated under photoheterotrophic conditions to compensate for loss of photosynthetically produced NADPH, but gene expression was again unaffected. In contrast to the previous study of Yang et al. (2002c), some residual oxPPP flux was still detectable under mixotrophic conditions. The authors attributed this to the lower light intensity used in the more recent study (40 vs.  $125 \mu\text{mol m}^{-2} \text{s}^{-1}$ ), consistent with model predictions reported by Shastri and Morgan (2005). The gene that exhibited the largest expression change was *gap1*, which encodes an isoform of glyceraldehyde-3-phosphate dehydrogenase (GAPDH) that is essential for glycolytic glucose breakdown and was suggested to respond to NADPH levels by shifting carbon flow between glycolysis and oxPPP.

Another recent study by You et al. (2014) confirmed conclusions from previous studies but also provided a new perspective on TCA cycle in *Synechocystis* 6803 under mixotrophic growth conditions. In addition to  $^{13}\text{C}$  MFA, isotope dilution experiments were performed to identify the presence of particular pathways. To accomplish this, cells were fully labeled using  $\text{NaH}^{13}\text{CO}_3$  and  $[\text{U}-^{13}\text{C}_6]$  glucose, after which unlabeled glyoxylate or glutamate was added to determine the activities of specific reactions. Similar to the flux analysis of Nakajima et al. (2014), this study calculated a zero flux through the glyoxylate shunt. The MFA

model yielded evidence of high malic enzyme activity in agreement with the previous analysis by Yang et al. (2002b). OxPPP flux was low under the light- and carbon-sufficient conditions of the early-exponential phase, but labeling in late-exponential phase indicated higher oxPPP activity. You et al. focused particular attention toward elucidating the direction and activity of the TCA cycle. Isotope dilution with glutamate detected carbon flow through  $\alpha$ -ketoglutarate to succinate, consistent with activity of the  $\alpha$ -ketoglutarate decarboxylase bypass pathway recently discovered by Zhang and Bryant (2011). However,  $^{13}\text{C}$  MFA verified that flux through this pathway was negligibly small, in agreement with previous MFA studies.

In addition to *Synechocystis*, other strains of cyanobacteria have also become the subject of recent flux profiling experiments. A steady-state  $^{13}\text{C}$  labeling study by Feng et al. (2010) investigated the effects of different carbon and nitrogen substrates on the central metabolism of *Cyanotrichia* sp. ATCC 51142 under continuous light conditions. Three labeled substrates were tested ( $[\text{U}-^{13}\text{C}]$  glucose,  $[2-^{13}\text{C}]$  glycerol, and  $[3-^{13}\text{C}]$  pyruvate) in either nitrogen-fixing or nitrogen-sufficient conditions to determine their impacts on growth and amino acid biosynthesis. GC–MS was used to analyze the  $^{13}\text{C}$  enrichment of five amino acids: histidine and serine, which are synthesized in the Calvin cycle and PPP; alanine, which is derived from pyruvate; and aspartate and glutamate, which are both TCA cycle derivatives (Fig. 2). Glycerol addition doubled the specific growth rate under both nitrogen-fixing and nitrogen-sufficient conditions, but neither glucose nor pyruvate enhanced growth in comparison to a control photoautotrophic culture. Consistent with this observation, the contribution of glycerol carbon to amino acid biosynthesis was substantially higher than either glucose or pyruvate. Furthermore, the amino acids histidine, alanine, and serine were completely derived from glycerol carbon under nitrogen-sufficient conditions, indicating a shift to photoheterotrophic growth. This study highlights the use of  $^{13}\text{C}$  labeling studies to reveal major pathways of carbon utilization in less characterized species.

Although Feng et al. (2010) made extensive use of  $^{13}\text{C}$  labeling data to determine the contributions of extracellular carbon substrates to intracellular amino acid pools, the authors did not attempt to estimate intracellular fluxes using rigorous pathway modeling. Another study by Alagesan et al. (2013) provided a more comprehensive flux analysis of *Cyanotrichia* sp. ATCC 51142 metabolism under similar growth conditions. A comparison of these two studies underscores the effects that culture conditions and measurement availability have on the computed fluxes. Both groups analyzed growth in nitrogen-sufficient and nitrogen-fixing conditions using  $^{13}\text{C}$ -labeled glycerol as a



carbon source. However, Feng et al. determined that a glycerol-fed culture in nitrogen-replete media exhibited photoheterotrophic growth in the presence of light, while Alagesan et al. observed mixotrophic metabolism under similar conditions. The variation in culture experimental setup likely caused this difference, as the latter group chose a higher light intensity (100 vs. 50  $\mu\text{mol m}^{-2} \text{s}^{-1}$ ) to avoid light limitation, and the cells were harvested early in the exponential growth phase to maintain sufficient  $\text{CO}_2$  availability. Also, a greater number of amino acids were analyzed by Alagesan et al., providing increased redundancy and pathway coverage. This enabled  $^{13}\text{C}$  MFA to be performed based on an extensive metabolic model that included a complete TCA cycle, as recently reported by Zhang and Bryant (2011). In both cases, the addition of glycerol to the media resulted in a higher growth rate, and both groups also noted incorporation of  $\text{CO}_2$  through anaplerotic pathways involved in the formation of oxaloacetate (OAA) from PEP (i.e., C4-like metabolism). Further evaluation of this strain would benefit from standardized growth conditions and also by extending the  $^{13}\text{C}$  MFA studies to include additional isotopomer measurements beyond those obtained from proteinogenic amino acids.

### $^{13}\text{C}$ INST-MFA

The development of software packages such as INCA has enabled INST-MFA studies of autotrophic metabolism in cyanobacteria, which complement previous studies that have been limited to heterotrophic or mixotrophic conditions. The approach was first applied by Young et al. (2011) to the model cyanobacterium *Synechocystis* 6803 growing in a controlled photobioreactor. The study relied on both GC–MS and LC–MS/MS to quantify labeling trajectories of 15 intracellular metabolites following administration of  $^{13}\text{C}$ -labeled bicarbonate to the culture (Fig. 3). This was the first comprehensive flux analysis performed based on isotope labeling data obtained in a fully autotrophic system. Steady-state labeling was typically achieved in less than 10 min, with the notable exception of TCA pathway intermediates (e.g., succinate, fumarate, and citrate) that were more slowly labeled. The flux map obtained using  $^{13}\text{C}$  INST-MFA was compared to a previously published linear programming (LP) solution that predicted the theoretical optimum flux profile needed to maximize growth and minimize light utilization (Shastri and Morgan 2005). Overall, the results indicated that photoautotrophically grown *Synechocystis* cells exhibited suboptimal carbon efficiency, with significant loss of fixed  $\text{CO}_2$  via oxPPP. This provides an example of how flux analysis can be used to identify pathways responsible for reduced productivity, by pinpointing wasteful processes

that contribute to carbon losses. These pathways offer potential metabolic engineering targets that can be manipulated to increase flux to desirable products.

Earlier that same year, Huege et al. (2011) published results from a transient  $^{13}\text{C}$  labeling study comparing wild-type *Synechocystis* and two photorespiratory pathway mutants pre-acclimated to either high carbon (HC) or low carbon (LC) conditions. Although the authors did not attempt to perform a comprehensive flux analysis, they were able to assess metabolite turnover and provide local flux estimates (e.g., sucrose production) based on the observed dynamics of total  $^{13}\text{C}$  enrichment. Despite differing growth and labeling conditions, the wild-type results were largely in agreement with the findings of Young et al. (2011). It was determined in both cases that activity of C3 metabolism involving RuBisCO was the primary source of carbon fixation, although C4 metabolism through PEP carboxylase (PEPC) was active to a lesser degree as noted in the *Cyanothece* studies (Feng et al. 2010; Alagesan et al. 2013). However, Huege et al. noted PEPC activity only in LC conditions, whereas Young et al. calculated flux in the equivalent of HC conditions. Both groups noted that RuBisCO oxygenase activity was very low in the wild-type strains. Also, the glyoxylate shunt was found to be inactive in both of these studies, as no evidence was found in the  $^{13}\text{C}$  labeling data to support its presence under photoautotrophic conditions. Lastly, both groups noted the possibility of metabolite channeling within pathways, where enzymes catalyzing successive reactions cluster together spatially in order to minimize diffusional limitations. This effect was revealed by more rapid  $^{13}\text{C}$  enrichment and higher steady-state labeling of some downstream metabolites relative to upstream metabolites, which could not be explained in the absence of metabolite channeling.

A similar transient  $^{13}\text{C}$  labeling study was recently combined with intracellular metabolite profiling to investigate the response to nitrate depletion in cyanobacteria (Hasunuma et al. 2013). In *Arthrospira platensis* and *Synechocystis* 6803, the rate of  $^{13}\text{C}$  incorporation in central carbon metabolites and amino acids was determined over a thirty-minute period of labeling with  $\text{NaH}^{13}\text{CO}_3$ . In comparison with cells grown under nitrogen-replete conditions, nitrogen depletion resulted in lower cell growth rate, lower percentage of proteins in the cell, and higher glycogen content. The  $^{13}\text{C}$  labeling data indicated that, with the exception of glutamine and glutamate, the enrichment of most intracellular metabolites was significantly decreased in *A. platensis* cells cultivated without nitrate. These findings suggest that cyanobacteria placed under nitrogen stress conditions degrade intracellular proteins to amino acids, which then serve as the carbon source for glycogen synthesis.

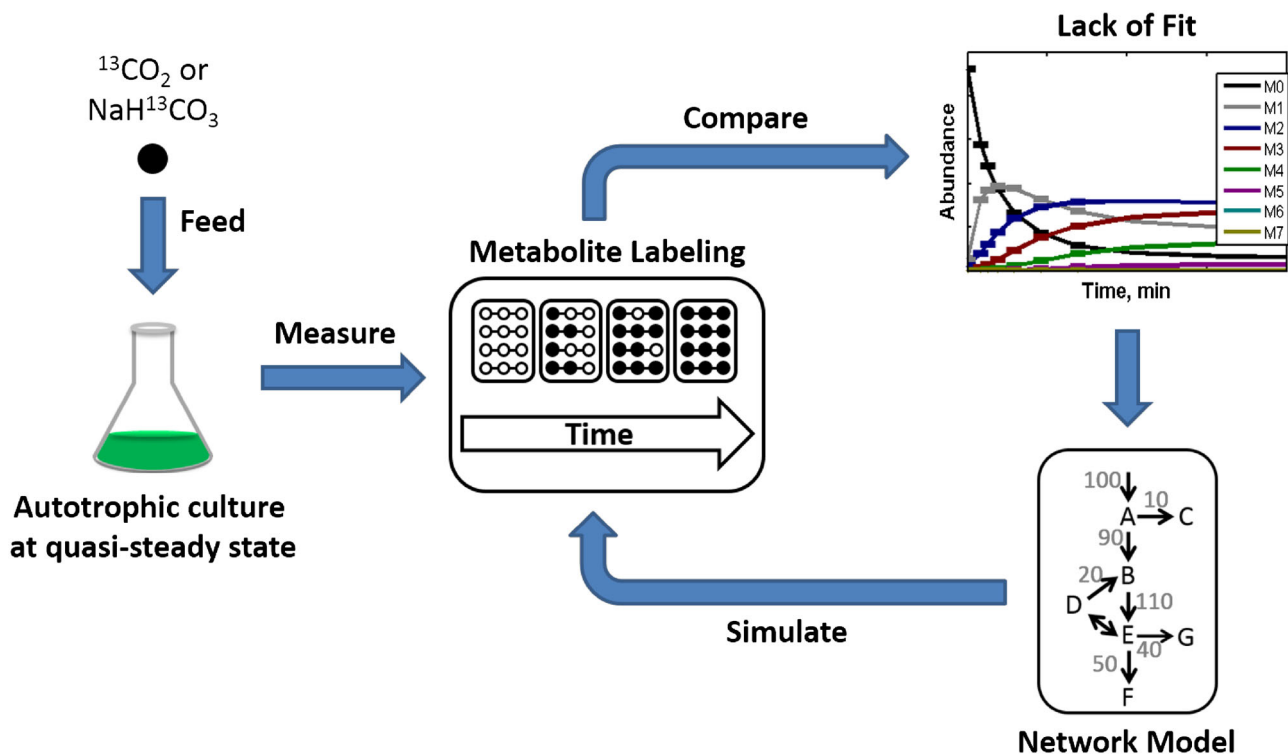


**Fig. 3** Workflow of INST-MFA in cyanobacteria. Labeled  $\text{CO}_2$  or bicarbonate is fed to a culture at metabolic (quasi-) steady state, and metabolite labeling is measured over time using mass spectrometry. The mass isotopomer distributions (MIDs) of all measured

metabolites are compared with simulated values produced by a mathematical model of the transient isotopomer balances. The fluxes in the model are iteratively adjusted until the simulated MIDs match their experimentally determined values

### Study design for $^{13}\text{C}$ INST-MFA of cyanobacteria

#### Measurement capabilities

In general, there are three types of measurements that are useful for INST-MFA studies, listed here in order of importance and discussed further below: (i) extracellular exchange rates, (ii) intracellular  $^{13}\text{C}$  labeling, and (iii) extracellular  $^{13}\text{C}$  labeling. Unlike related approaches such as kinetic flux profiling (Yuan et al. 2008), direct measurements of intracellular metabolite pool sizes are not essential for flux estimation by INST-MFA (Young et al. 2011). The pool sizes are treated as adjustable model parameters, which are optimized to match the experimental labeling dynamics during the data regression. This is a significant advantage of INST-MFA over other modeling approaches that depend explicitly on pool size measurements or kinetic parameters not reliably known in vivo. While pool size measurements can be provided to the data regression as a way to further improve flux resolution, it is often difficult to achieve absolute quantification of intracellular pool sizes due to losses during metabolite extraction or unknown subcellular

compartmentalization of reactions. Furthermore, we have learned from experience that precise flux estimates can be obtained without provision of direct pool size measurements. Therefore, we have avoided the potential biases that may be introduced by including pool size measurements in our INST-MFA calculations but instead have used them to independently validate the model-derived estimates.

To further examine the effects of pool size measurements on estimated fluxes, we used our previous metabolic model of *Synechocystis* 6803 and treated the pool size estimates determined by INST-MFA as if they were directly measured values, assuming 10 % relative errors. From this simulated dataset, we computed a contribution matrix based on local parameter sensitivities (Antoniewicz et al. 2006). The contribution heat map (Fig. 4) shows that the MS labeling measurements were most important for determining the values of the net and exchange fluxes, while the pool size measurements made negligible contributions toward flux determination. Therefore, the availability of direct pool size measurements would not be expected to significantly improve the precision of flux estimates obtainable with this model.

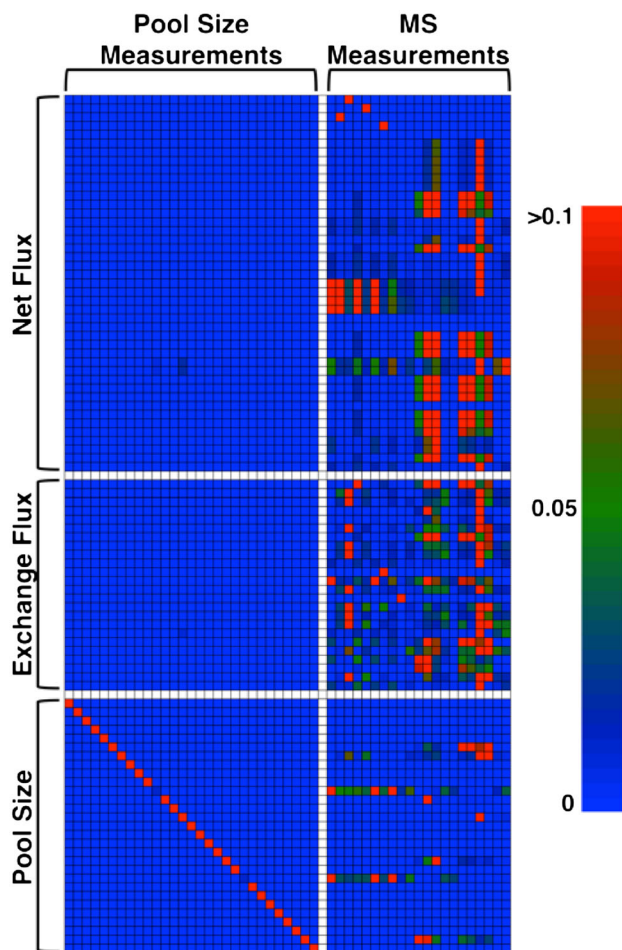


**Fig. 4** Heat map showing contributions of pool size and isotopic labeling measurements to estimated parameters. Each element of this contribution matrix (e.g., at row  $i$  and column  $j$ ) represents the fractional contribution of the  $j$ th measurement to the local variance of the  $i$ th parameter. The contribution values in each row sum to unity

#### Extracellular flux measurements

Measurement of extracellular exchange rates is required to constrain the carbon inputs and outputs to the metabolic network. For soluble metabolites, this involves measuring the depletion of carbon substrates and the accumulation of carbon products in extracellular medium samples collected over time, followed by regression analysis to assess the uptake/excretion rates of these metabolites (Murphy and Young 2013). Cell-free medium samples should be analyzed in parallel to control for medium evaporation or metabolite degradation. For gas compounds, it is often necessary to use specialized equipment such as a gas analyzer or online mass spectrometer to measure exchange rates based on analysis of culture off-gas. Furthermore, a cold-trap may be necessary to accurately quantify the formation rate of highly volatile products such as short-chain alcohols or aldehydes. Typically, if there are  $N$  exchange

rates, at least  $N-1$  of these should be measured to fully constrain the model (the remaining exchange rate can always be determined based on the overall carbon balance). For autotrophic growth of cyanobacteria, this means that  $\text{CO}_2$  uptake must be measured in combination with the production rates of all but one major carbon product. Alternatively, the  $\text{CO}_2$  uptake measurement could be dropped if all major carbon products are measured. Some minor products can be neglected, depending on the accuracy desired, if they are considered to contribute insignificantly to the overall carbon balance.

#### Intracellular isotopomer measurements

To fully constrain the intracellular fluxes, it is also necessary to supply measurements of  $^{13}\text{C}$  isotope labeling to the model. In our previously published study (Young et al. 2011) on the central metabolism of *Synechocystis* 6803, we used a combination of LC-MS/MS and GC-MS to quantify isotope labeling in several sugar phosphate and organic acid metabolites following a pulse of 50 %  $\text{NaH}^{13}\text{CO}_3$ . While NMR can also be applied to obtain direct information on position-specific  $^{13}\text{C}$  labeling, its lower sensitivity and throughput have limited its use primarily to steady-state  $^{13}\text{C}$  MFA studies that rely on measurements of proteinogenic amino acids rather than free intracellular metabolites.

The precision of flux estimates obtained from INST-MFA is dependent upon the measurement of metabolite labeling within the pathways of interest. In order to assess the relative importance of the measurements included in our prior study (Young et al. 2011), we used the same model and flux estimates to simulate time-course mass isotopomer measurements at the times listed in Table 1. We then estimated best-fit model parameters using the full complement of MS measurements and assuming 0.5 mol % uncertainties on all values (base case model). Next, we separated all mass isotopomer measurements into one of six groups based on their location within the metabolic network, as shown in Table 2, and re-estimated fluxes after inactivating each group one-at-a-time. As expected, inactivating measurements did not change the best-fit values of the estimated fluxes, but their estimated uncertainties were significantly increased in several cases. To precisely quantify flux uncertainties, we computed 95 % confidence intervals (CIs) for six net fluxes, which together span the null space of the stoichiometric matrix and are therefore representative of all independent degrees of freedom: G6P dehydrogenase (G6PDH), part of oxPPP; RuBisCO carboxylase (RBC) and SBPase (SBP), both part of the CBB cycle; RuBisCO oxygenase (RBCOX), part of the photorespiratory (PR) pathway; malic enzyme (ME), part of the PEP cycle; and malate synthase (MS), part of the glyoxylate shunt. Figure 5 shows the fold change in



**Table 1** Time points chosen for simulation of mass isotopomer measurements

Exponentially spaced time points were simulated as suggested by Nöh and Wiechert (2006):  $t_i = ab^{i-1}$  for  $i = 1, 2, \dots, n$ , where  $t_1 = a = 20$  s,  $n = 10$ , and  $t_n = 900$  s. The exact times calculated using this formula were rounded to the values shown

$i$	$T_i$ (s)
1	20
2	30
3	45
4	70
5	110
6	165
7	250
8	390
9	590
10	900

uncertainty for these six fluxes after inactivating each measurement group. A group was considered to significantly contribute to the identifiability of a particular flux if the flux's uncertainty increased by more than 1.5-fold in response to inactivation of the group. Any groups considered significant based on this criterion were further examined by inactivating each individual metabolite within the group one-at-a-time to determine which contributed the most toward the observed change in uncertainty.

The results from the flux uncertainty analysis fell into natural groupings as shown in Fig. 5. The uncertainties of G6PDH, RBC, and RBCOX fluxes increased by 1.5- to 1.6-fold upon deactivation of the CBB-5C/7C group, yet further analysis showed that this was a cumulative effect of all four metabolites included in the group, rather than one specific metabolite. Additionally, the uncertainties of G6PDH and RBC nearly doubled with the inactivation of the G6P measurement, and RBCOX quadrupled by the inactivation of the PR pathway metabolite glycerate. The second grouping contained the fluxes ME and MS, for which significant changes were observed upon inactivation of the TCA pathway measurements (over 5-fold and 2-fold, respectively) and PEP cycle measurements (over 1.5-fold and 2.5-fold, respectively). Citrate contributed the most

toward the importance of the TCA group, although no single measurement within this group was responsible for the entirety of the observed effect on either ME or MS. Inactivation of MAL alone led to a nearly 2.5-fold increase in the ME uncertainty and over a 1.5-fold change in the MS uncertainty. Furthermore, inactivation of glycerate measurements led to an almost 4-fold increase in the MS uncertainty, likely because the substrate of this enzyme, glyoxylate, is also an intermediate in the PR pathway. The uncertainty of the remaining flux, SBP, was most strongly affected by the inactivation of the two CBB cycle groups. In this case, the change induced by dropping the CBB-3C/6C group was most affected by DHAP (1.6-fold increase), while the response to dropping the CBB-5C/7C group was more clearly due to inactivation of the S7P measurement (7-fold increase).

We also investigated the effects of varying the timing of sample collections by inactivating different measurement time points and re-estimating uncertainties for the same six independent fluxes (Fig. 6). Although most flux estimates were robust to dropping a few evenly spaced time points, the identifiability of the SBP flux was affected quite strongly by evenly spaced removal of time points, increasing nearly 2-fold upon inactivation of odd time points. This appears to be largely due to loss of information at the early time points, since dropping all time points in the range under 2 min ( $i = 1-5$ ) caused the SBP flux uncertainty to increase almost 4-fold. On the other hand, the other five fluxes were more strongly affected by inactivation of the late time points ( $i = 6-10$ ). This is likely due to the fact that insufficient labeling was obtained in some slowly labeled metabolites (e.g., TCA cycle intermediates) to adequately constrain the flux solution based on the early time points alone. Predictably, inactivation of all but three time points ( $i = 4, 7, \text{ and } 10$ ) resulted in increased uncertainty of all fluxes, although the effect on SBP was more dramatic.

**Table 2** List of simulated ion fragments

CBB-3C/6C (G1)	CBB-5C/7C (G2)	TCA (G3)	PEP-cyc (G4)	PR (G5)	OXPPP (G6)
3PGA185 (1.1)	R5P229 (2.1)	SUC247 (3.1)	PEP167 (4.1)	GA292	G6P259
3PGA357 (1.1)	RUBP309 (2.2)	FUM245 (3.2)	MAL233 (4.2)	GA307	
3PGA459 (1.1)	S7P289 (2.3)	CIT273 (3.3)			
DHAP169 (1.2)	RU5P229 (2.4)	CIT363 (3.3)			
F6P259 (1.3)		CIT375 (3.3)			
GAP169 (1.4)		CIT465 (3.3)			

The measured ions were divided into one of six groups based on pathway location and size. The six groups contain CBB cycle 3- and 6-carbon metabolites, CBB cycle 5- and 7-carbon metabolites, TCA pathway metabolites, PEP cycle metabolites, PR pathway metabolites, and oxPPP metabolites. The groups were numbered as shown in parentheses, and in the case of G1–G4, ions representing individual metabolites were also organized into numbered subgroups

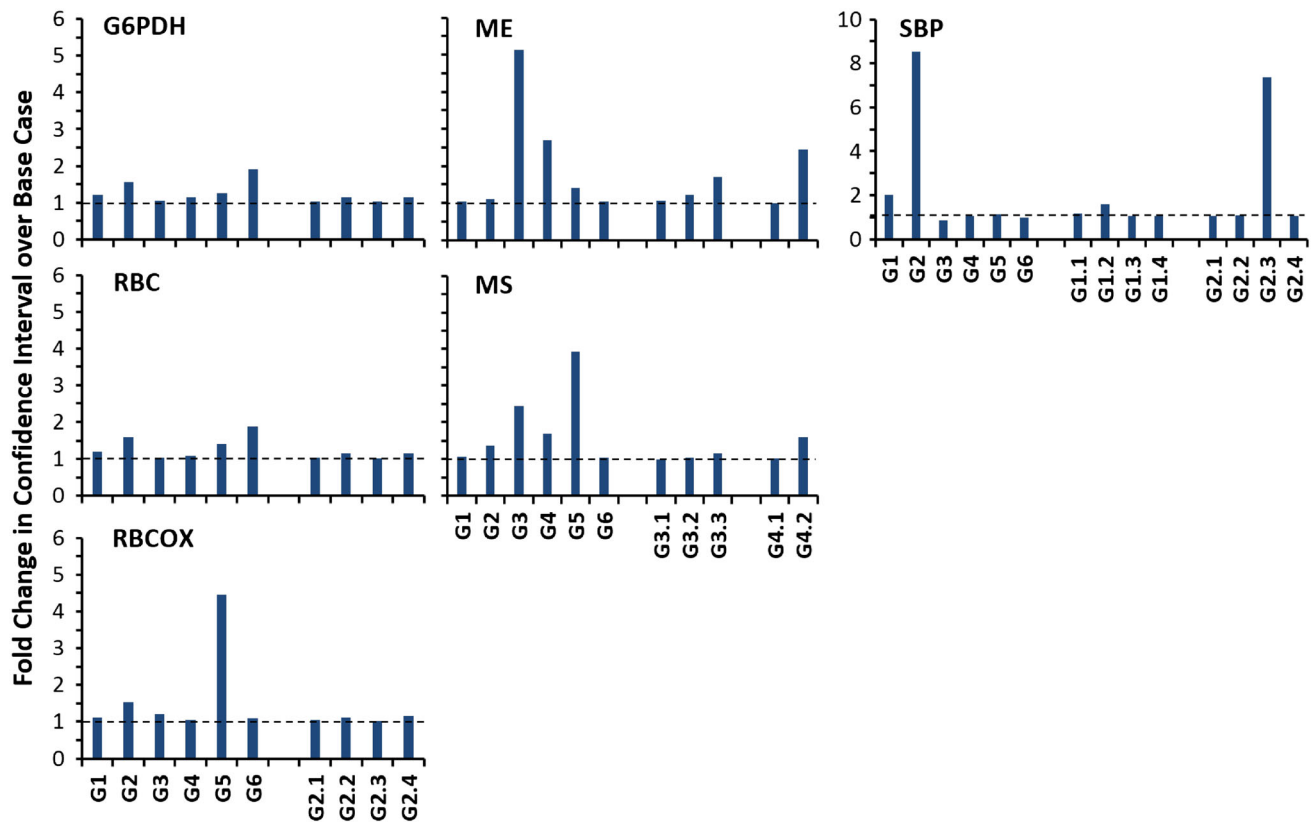


**Fig. 5** Effect of removing measurements on flux uncertainties. Groups of measurements (G1–G6) were inactivated in the model, and the 95 % confidence interval (CI) width for each of six independent fluxes was recalculated and compared to the base case model, which includes all measurements examined by Young et al.

(2011). If the CI width increased by more than 1.5-fold, the analysis was repeated for each individual metabolite in the group to determine which one(s) contributed most to the observed increase. See Table 2 for a list of measurements included in each group

### Extracellular isotopomer measurements

Measurement of isotope labeling in extracellular products is typically unnecessary since their labeling simply reflects the slow accumulation of material derived from a more rapidly labeled intracellular pool. These measurements can provide consistency checks on the intracellular measurements, but usually do not contribute important new information. On the other hand, it is important to estimate the labeling of the tracer substrate itself, which could be  $^{13}\text{CO}_2$  or  $\text{NaH}^{13}\text{CO}_3$  in photoautotrophic studies. This could be estimated based on labeling measurements of CBB intermediates obtained at long time points (after the system reaches isotopic steady state), since the  $^{13}\text{C}$  enrichment of intracellular metabolites should asymptotically approach the tracer enrichment at these times. However, this estimate could be biased downward if there are metabolically inactive (i.e., “cold”) pools that do not fully label even at long times. Therefore, it would be useful to directly measure the enrichment of extracellular bicarbonate, although this has not been done in previous INST-MFA studies. If necessary, the model can account for the dynamics of

tracer mixing by including an extracellular bicarbonate pool that gradually equilibrates with the tracer.

### Experimental design

Cell culture experiments should be designed to mimic the physiological conditions of interest as closely as possible, in order to maximize the relevance of the MFA results. Due to the substantial biological variance existing within many organisms, the Metabolomics Standards Initiative has recommended a minimum of triplicate ( $n = 3$ ) biological sampling and analyses, with  $n = 5$  preferred (Sumner et al. 2007). Measurement of extracellular exchange rates can be performed using parallel experiments in the absence of isotope tracers, or extracellular samples can be collected from the ILEs to enable simultaneous measurement of exchange rates and  $^{13}\text{C}$  enrichments from the same culture. Prior to administering the  $^{13}\text{C}$  tracer, the culture metabolism should have reached a stable quasi-steady state (QSS). This is typically achieved during exponential growth of cell cultures. Non-exponential cultures can also achieve QSS metabolism as long as they are not experiencing rapid

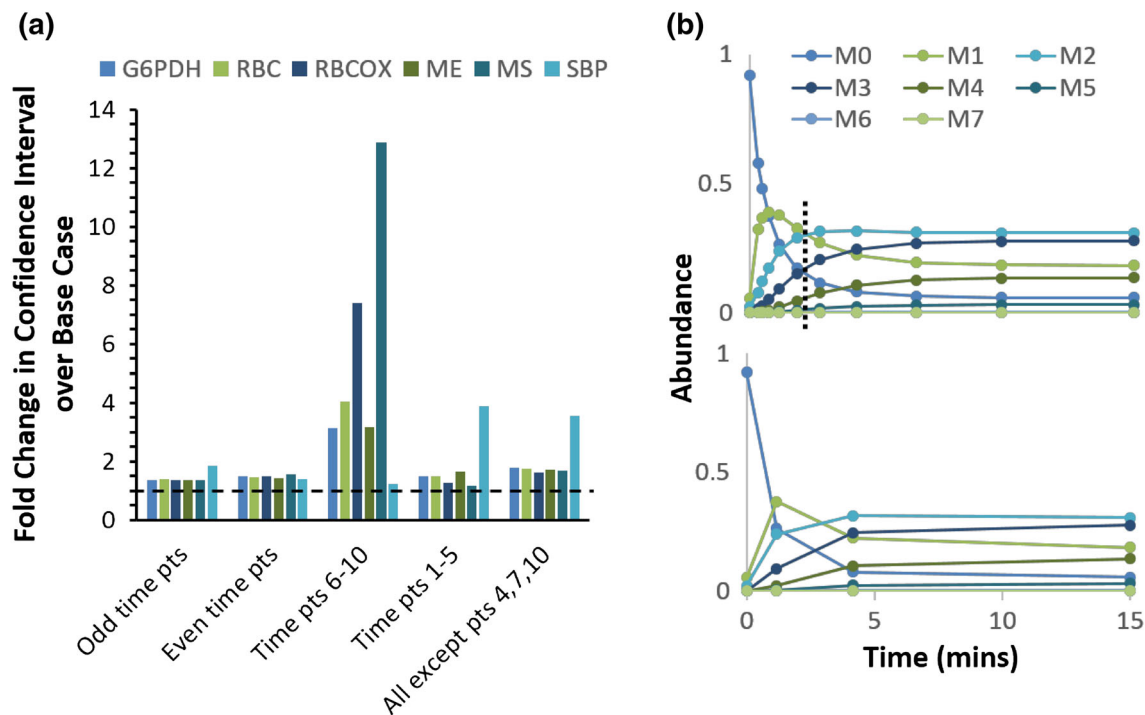


**Fig. 6** Effect of removing time points on flux uncertainties. **a** Using data simulated from the base case model, groups of time points were inactivated as indicated to examine their effect on the CI width of six independent fluxes. **b** Transient metabolite labeling data for

RUBP309 is shown as an example of the base case, with a *dotted line* to separate time points 1–5 from time points 6–10 (*upper*), and of time points 4, 7, and 10 only (*lower*)

changes in growth rate or nutrient levels (i.e., any changes in metabolism are slow relative to the time scale of the isotope labeling experiment). However, in these cases, it may be desirable to perform the labeling experiments in continuous mode (i.e., in a chemostat or turbidostat) to achieve maximum control and reproducibility. This would ensure that the cultures are experiencing the same growth rate and turbidity during each replicate experiment and will also enable the culture to be maintained in a fixed QSS for extended periods of time. The main drawback is that continuous cultures are more complicated to operate and may not accurately represent the growth conditions of interest for bioprocess applications.

Once the QSS to be studied has been established, either  $^{13}\text{CO}_2$  or  $\text{NaH}^{13}\text{CO}_3$  can be introduced to the culture.  $\text{NaH}^{13}\text{CO}_3$  can be introduced directly into the culture medium as a bolus (in batch mode) or as a prime-constant infusion (in continuous mode).  $^{13}\text{CO}_2$  can be introduced by switching the gas feed to a tracer mixture with identical chemical composition but with unlabeled  $\text{CO}_2$  replaced by  $^{13}\text{CO}_2$ . In either case, care should be taken not to disturb the previously established metabolic QSS. One advantage of using a  $^{13}\text{CO}_2$  gas feed is that unlabeled carbon will be rapidly washed out of the culture and replaced by the tracer. Shastri and Morgan (2007) have performed computational simulations, which demonstrate that an immediate step change in the enrichment

of dissolved  $\text{CO}_2$  is possible by selecting proper operating conditions that account for the volumetric gas–liquid mass transfer coefficient and composition of air (i.e.,  $\%\text{CO}_2$ ) fed to the system. This labeling method enables the study of either light-limited or  $\text{CO}_2$ -limited cultures. If feeding  $\text{NaH}^{13}\text{CO}_3$ , bicarbonate should already be at saturating levels so that the additional  $\text{NaH}^{13}\text{CO}_3$  bolus will not alter metabolism. In this case, it is only possible to study light-limited cultures without disturbing the QSS. Also, a significant amount of  $\text{NaH}^{13}\text{CO}_3$  will need to be added to achieve adequate  $^{13}\text{C}$  enrichment of the extracellular bicarbonate pool, since the tracer will be diluted by the pre-existing unlabeled bicarbonate in the medium. In our prior studies, we have found that at least 50 % enrichment of the extracellular bicarbonate pool is sufficient for precise flux estimation, although lower enrichments have not been rigorously assessed.

Once the tracer has been introduced, a time series of cell and medium samples should be collected at 5–10 time points spanning 20 min to 1 h. The culture should be sampled more frequently at early time points when labeling is changing most rapidly (Noh and Wiechert 2006). Longer time points (i.e., 1 h or longer), however, provide additional information especially useful for metabolites with low turnover rates, such as those in the TCA cycle. The biomass samples should be rapidly cold-quenched using a low-temperature solution and centrifuged or filtered to

remove the spent medium (Krall et al. 2009). Then, the cell pellet can be flash-frozen in liquid nitrogen or can proceed directly into the metabolite extraction protocol. Culture medium samples do not need to be rapidly cold-quenched but instead can be centrifuged to remove cells and then frozen for later analysis. If  $^{13}\text{C}$  flux analysis is to be performed at multiple time points during the growth cycle, it is recommended to use parallel replicate cultures and introduce the tracer to each culture at different times, rather than labeling the same culture repeatedly. The INCA program is currently only able to describe experiments that begin with an unlabeled (i.e., naturally labeled) culture at the time the tracer is introduced, so repeatedly labeling the same culture is not amenable to analysis.

### Computational resources

In addition to the experimental requirements for INST-MFA, there is also a substantial computational component. This involves developing a mathematical model of the differential mass and isotopomer balances that describe the flow of carbon through the metabolic network. The INCA software package automates the development and solution of these balance equations (Young 2014). However, significant user input is still required (i) to identify the proper reaction equations and specify metabolite properties, (ii) to supply experimental measurements and tracer information to the model, (iii) to investigate and resolve points of disagreement between the model simulations and the experimental measurements, and (iv) to assess the quality of the results and provide biological interpretation. In addition to software, a small Beowulf computer cluster can be used to speed up long-running computations. Although many types of INST-MFA calculations can be performed on a single computer, some types of calculations (e.g., sensitivity analysis to determine parameter uncertainties) can take several days if not parallelized. INCA has built-in capabilities for parallelization of certain time-consuming processes, which can be invoked within a cluster computing framework. Our lab currently uses a cluster of eight quad-core Dell desktop computers running the Rocks 6.0 Linux distribution (<http://www.rocksclusters.org>). INCA can use either the MATLAB Distributed Computing Server with Parallel Computing Toolbox or the Condor job scheduler (pre-packaged with Rocks) to distribute jobs to compute nodes within the cluster.

### Conclusions & future outlook

$^{13}\text{C}$  MFA has emerged as an important platform to extract otherwise unobservable information about metabolic

pathway fluxes through inference from experimental measurements. While the models used for MFA are not intended to be predictive on their own, the information they provide can be used to develop and validate other types of models (either stoichiometric or kinetic models) that possess predictive capabilities. Furthermore, the direct insight derived from viewing a flux map can itself often lead to intuitive predictions about pathway operation. Comparison of flux maps obtained under varying experimental conditions or in the presence of targeted genetic manipulations provides a functional readout on the global impact that these perturbations have on cell metabolism. This information can be used to identify rigid nodes, which resist change when neighboring enzymes are manipulated, and flexible nodes that are amenable to easy modulation. Such knowledge is critical for rational selection of metabolic engineering targets.

While much prior work has focused on the development of stoichiometric MFA models in cyanobacteria, and in fact several genome-scale metabolic reconstructions are now becoming available, the major disadvantage of these models is that they cannot provide a unique flux solution unless a cellular growth objective is postulated (e.g., as in flux balance analysis, or FBA). In this case, it is important to note that the flux solution obtained from FBA does not represent the actual flux distribution within the system but instead a theoretical solution predicted to optimize growth. Therefore, even when FBA predictions are available, performing  $^{13}\text{C}$  MFA studies can pinpoint unexpected deviations between theoretically and experimentally determined fluxes that indicate suboptimal pathway function or a lack of understanding about pathway operation. While some prior studies have found satisfactory agreement between the two types of flux solutions, others have noted significant disagreements between the two (Schuetz et al. 2007; Young et al. 2011). Indeed, it is precisely these disagreements between theory and experiment that often suggest new discoveries, thus highlighting the potential for  $^{13}\text{C}$  MFA to expand our understanding of cyanobacterial metabolism. Realizing this potential requires continued development of experimental protocols and computational tools that facilitate the application of  $^{13}\text{C}$  MFA to a wider range of cyanobacterial strains and growth conditions. The recent emergence of the INST-MFA approach, along with enabling software such as INCA, provides a significant example of how  $^{13}\text{C}$  MFA is expanding its reach to encompass new experimental systems (e.g., autotrophic cultures) that were not previously amenable to study.

**Acknowledgments** This project was supported by the U.S. Department of Energy (DOE) Award DE-SC008118 and the U.S. Department of Education Graduate Assistance in Areas of National



Need Award P200A090323. LJJ was supported by the DOE Office of Science Graduate Fellowship DE-AC05-06OR23100.

## References

- Alagesan S, Gaudana SB, Sinha A, Wangikar PP (2013) Metabolic flux analysis of *Cyanothece* sp. ATCC 51142 under mixotrophic conditions. *Photosynth Res* 118(1–2):191–198. doi:10.1007/s11120-013-9911-5
- Antoniewicz MR (2013) 13C metabolic flux analysis: optimal design of isotopic labeling experiments. *Curr Opin Biotechnol* 2013(24):1116–1121
- Antoniewicz MR, Kelleher JK, Stephanopoulos G (2006) Determination of confidence intervals of metabolic fluxes estimated from stable isotope measurements. *Metab Eng* 8(4):324–337. doi:10.1016/j.ymben.2006.01.004
- Antoniewicz MR, Kelleher JK, Stephanopoulos G (2007a) Elementary metabolite units (EMU): a novel framework for modeling isotopic distributions. *Metab Eng* 9(1):68–86. doi:10.1016/j.ymben.2006.09.001
- Antoniewicz MR, Kraynie DF, Laffend LA, Gonzalez-Lergier J, Kelleher JK, Stephanopoulos G (2007b) Metabolic flux analysis in a nonstationary system: fed-batch fermentation of a high yielding strain of *E. coli* producing 1,3-propanediol. *Metab Eng* 9(3):277–292. doi:10.1016/j.ymben.2007.01.003
- Araújo-Bravo MJ, Shimizu K (2003) An improved method for statistical analysis of metabolic flux analysis using isotopomer mapping matrices with analytical expressions. *J Biotechnol* 105(1–2):117–133. doi:10.1016/S0168-1656(03)00169-X
- Berla BM, Saha R, Immethun CM, Maranas CD, Moon TS, Pakrasi HB (2013) Synthetic biology of cyanobacteria: unique challenges and opportunities. *Frontiers Microbiol* 4:246. doi:10.3389/fmicb.2013.00246
- Feng X, Bandyopadhyay A, Berla B, Page L, Wu B, Pakrasi HB, Tang YJ (2010) Mixotrophic and photoheterotrophic metabolism in *Cyanothece* sp. ATCC 51142 under continuous light. *Microbiology* 156(8):2566–2574. doi:10.1099/mic.0.038232-0
- Hasunuma T, Kikuyama F, Matsuda M, Aikawa S, Izumi Y, Kondo A (2013) Dynamic metabolic profiling of cyanobacterial glycogen biosynthesis under conditions of nitrate depletion. *J Exp Bot* 64(10):2943–2954. doi:10.1093/jxb/ert134
- Huege J, Goetze J, Schwarz D, Bauwe H, Hagemann M, Kopka J (2011) Modulation of the major paths of carbon in photorespiratory mutants of *synechocystis*. *PLoS One* 6(1):e16278
- Jazmin LJ, Young JD (2013) Isotopically nonstationary 13C metabolic flux analysis. In: Alper HS (ed) *Systems metabolic engineering*, vol 985., *Methods in molecular biology/Humana Press*, Totowa, pp 367–390. doi:10.1007/978-1-62703-299-5\_18
- Jazmin LJ, O’Grady JP, Ma F, Allen DK, Morgan JA, Young JD (2014) Isotopically nonstationary MFA (INST-MFA) of autotrophic metabolism. In: Dieuaide-Noubhani M, Alonso AP (eds) *Plant metabolic flux analysis*, vol 1090., *Methods in molecular biology/Humana Press*, Totowa, pp 181–210. doi:10.1007/978-1-62703-688-7\_12
- Koffas M, Stephanopoulos G (2005) Strain improvement by metabolic engineering: lysine production as a case study for systems biology. *Curr Opin Biotechnol* 16(3):361–366. doi:10.1016/j.copbio.2005.04.010
- Krall L, Huege J, Catchpole G, Steinhauser D, Willmitzer L (2009) Assessment of sampling strategies for gas chromatography-mass spectrometry (GC-MS) based metabolomics of cyanobacteria. *J Chromatogr B Analyt Technol Biomed Life Sci* 877(27):2952–2960. doi:10.1016/j.jchromb.2009.07.006
- Matsuoka Y, Shimizu K (2010) Current status of <sup>13</sup>C-metabolic flux analysis and future perspectives. *Process Biochem* 45(12):1873–1881. doi:10.1016/j.procbio.2010.03.025
- Murphy TA, Young JD (2013) ETA: robust software for determination of cell specific rates from extracellular time courses. *Biotechnol Bioeng* 110(6):1748–1758. doi:10.1002/bit.24836
- Nakajima T, Kajihata S, Yoshikawa K, Matsuda F, Furusawa C, Hirasawa T, Shimizu H (2014) Integrated Metabolic flux and omics analysis of *Synechocystis* sp. PCC 6803 under mixotrophic and photoheterotrophic conditions. *Plant cell physiol.* doi:10.1093/pcp/pcu091
- Nielsen J (2003) It is all about metabolic fluxes. *J Bacteriol* 185(24):7031–7035
- Noh K, Wiechert W (2006) Experimental design principles for isotopically stationary 13C labeling experiments. *Biotechnol Bioeng* 94(2):234–251. doi:10.1002/bit.20803
- Pelroy RA, Rippka R, Stanier RY (1972) Metabolism of glucose by unicellular blue-green algae. *Arch Mikrobiol* 87(4):303–322
- Sauer U (2006) Metabolic networks in motion: 13C-based flux analysis. *Mol Syst Biol.* doi:10.1038/msb4100109
- Schuetz R, Kuepfer L, Sauer U (2007) Systematic evaluation of objective functions for predicting intracellular fluxes in *Escherichia coli*. *Mol Syst Biol.* doi:10.1038/msb4100162
- Shastri AA, Morgan JA (2005) Flux balance analysis of photoautotrophic metabolism. *Biotechnol Prog* 21(6):1617–1626. doi:10.1021/bp050246d
- Shastri AA, Morgan JA (2007) A transient isotopic labeling methodology for 13C metabolic flux analysis of photoautotrophic microorganisms. *Phytochemistry* 68(16–18):2302–2312. doi:10.1016/j.phytochem.2007.03.042
- Stephanopoulos G (1999) Metabolic fluxes and metabolic engineering. *Metab Eng* 1:1–11
- Sumner L, Amberg A, Barrett D, Beale M, Beger R, Daykin C, Fan TM, Fiehn O, Goodacre R, Griffin J, Hankemeier T, Hardy N, Harnly J, Higashi R, Kopka J, Lane A, Lindon J, Marriott P, Nicholls A, Reilly M, Thaden J, Viant M (2007) Proposed minimum reporting standards for chemical analysis. *Metabolomics* 3(3):211–221. doi:10.1007/s11306-007-0082-2
- Tang YJ, Martin HG, Myers S, Rodriguez S, Baidoo EEK, Keasling JD (2009) Advances in analysis of microbial metabolic fluxes via C-13 isotopic labeling. *Mass Spectrom Rev* 28(2):362–375. doi:10.1002/Mas.20191
- Vallino JJ, Stephanopoulos G (1994) Carbon flux distributions at the pyruvate branch point in *Corynebacterium glutamicum* during lysine overproduction. *Biotechnol Progr* 10(3):320–326. doi:10.1021/Bp00027a013
- Wiechert W (2001) 13C metabolic flux analysis. *Metab Eng* 3(3):195–206. doi:10.1006/mben.2001.0187
- Wiechert W, Mollney M, Isermann N, Wurzel M, de Graaf AA (1999) Bidirectional reaction steps in metabolic networks: III. Explicit solution and analysis of isotopomer labeling systems. *Biotechnol Bioeng* 66(2):69–85
- Woolston BM, Edgar S, Stephanopoulos G (2013) Metabolic engineering: past and future. *Annual review of chemical and biomolecular engineering* 4:259–288. doi:10.1146/annurev-chembioeng-061312-103312
- Yang C, Hua Q, Shimizu K (2002a) Integration of the information from gene expression and metabolic fluxes for the analysis of the regulatory mechanisms in *Synechocystis*. *Appl Microbiol Biotechnol* 58(6):813–822. doi:10.1007/s00253-002-0949-0
- Yang C, Hua Q, Shimizu K (2002b) Metabolic flux analysis in *Synechocystis* using isotope distribution from 13C-labeled glucose. *Metab Eng* 4(3):202–216. doi:10.1006/mben.2002.0226
- Yang C, Hua Q, Shimizu K (2002c) Quantitative analysis of intracellular metabolic fluxes using GC-MS and two-dimensional NMR spectroscopy. *J Biosci Bioeng* 93(1):78–87

- You L, Berla B, He L, Pakrasi HB, Tang YJ (2014)  $^{13}\text{C}$ -MFA delineates the photomixotrophic metabolism of *Synechocystis* sp. PCC 6803 under light- and carbon-sufficient conditions. *Biotechnol J* 9(5):684–692. doi:[10.1002/biot.201300477](https://doi.org/10.1002/biot.201300477)
- Young JD (2014) INCA: a computational platform for isotopically non-stationary metabolic flux analysis. *Bioinformatics*. doi:[10.1093/bioinformatics/btu015](https://doi.org/10.1093/bioinformatics/btu015)
- Young JD, Walther JL, Antoniewicz MR, Yoo H, Stephanopoulos G (2008) An elementary metabolite unit (EMU) based method of isotopically nonstationary flux analysis. *Biotechnol Bioeng* 99(3):686–699. doi:[10.1002/bit.21632](https://doi.org/10.1002/bit.21632)
- Young JD, Shastri AA, Stephanopoulos G, Morgan JA (2011) Mapping photoautotrophic metabolism with isotopically non-stationary  $^{13}\text{C}$  flux analysis. *Metab Eng* 13(6):656–665. doi:[10.1016/j.ymben.2011.08.002](https://doi.org/10.1016/j.ymben.2011.08.002)
- Yuan J, Bennett BD, Rabinowitz JD (2008) Kinetic flux profiling for quantitation of cellular metabolic fluxes. *Nat Protoc* 3(8):1328–1340. doi:[10.1038/nprot.2008.131](https://doi.org/10.1038/nprot.2008.131)
- Zhang S, Bryant DA (2011) The tricarboxylic acid cycle in cyanobacteria. *Science* 334(6062):1551–1553. doi:[10.1126/science.1210858](https://doi.org/10.1126/science.1210858)